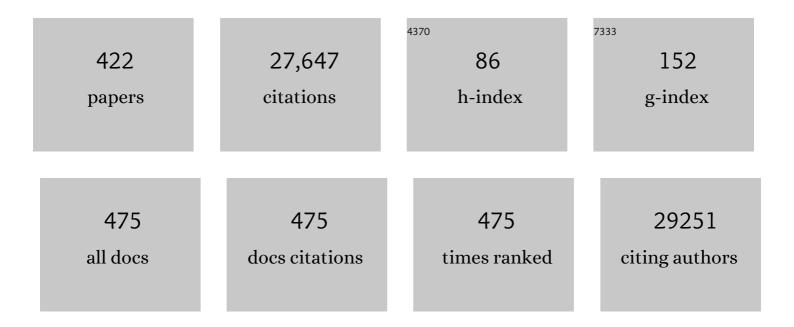
List of Publications by Year in descending order

Source: https://exaly.com/author-pdf/4802393/publications.pdf Version: 2024-02-01



#	Article	IF	CITATIONS
1	Ultra-small fluorescent metal nanoclusters: Synthesis and biological applications. Nano Today, 2011, 6, 401-418.	6.2	1,345
2	Engineered nanoparticles interacting with cells: size matters. Journal of Nanobiotechnology, 2014, 12, 5.	4.2	1,030
3	Surface Functionalization of Nanoparticles with Polyethylene Glycol: Effects on Protein Adsorption and Cellular Uptake. ACS Nano, 2015, 9, 6996-7008.	7.3	717
4	A quantitative fluorescence study of protein monolayer formation on colloidal nanoparticles. Nature Nanotechnology, 2009, 4, 577-580.	15.6	673
5	EosFP, a fluorescent marker protein with UV-inducible green-to-red fluorescence conversion. Proceedings of the National Academy of Sciences of the United States of America, 2004, 101, 15905-15910.	3.3	642
6	Differential Uptake of Functionalized Polystyrene Nanoparticles by Human Macrophages and a Monocytic Cell Line. ACS Nano, 2011, 5, 1657-1669.	7.3	516
7	Isothermal titration calorimetry. Analytical Chemistry, 1990, 62, 950A-959A.	3.2	482
8	Polymer-Coated Nanoparticles Interacting with Proteins and Cells: Focusing on the Sign of the Net Charge. ACS Nano, 2013, 7, 3253-3263.	7.3	477
9	Protein corona formation around nanoparticles – from the past to the future. Materials Horizons, 2014, 1, 301-313.	6.4	464
10	Ligand binding and conformational motions in myoglobin. Nature, 2000, 404, 205-208.	13.7	394
11	Ligand binding to heme proteins: connection between dynamics and function. Biochemistry, 1991, 30, 3988-4001.	1.2	392
12	Intracellular Thermometry by Using Fluorescent Gold Nanoclusters. Angewandte Chemie - International Edition, 2013, 52, 11154-11157.	7.2	357
13	Impact of Protein Modification on the Protein Corona on Nanoparticles and Nanoparticle–Cell Interactions. ACS Nano, 2014, 8, 503-513.	7.3	347
14	Oneâ€Pot Synthesis of Nearâ€Infrared Fluorescent Gold Clusters for Cellular Fluorescence Lifetime Imaging. Small, 2011, 7, 2614-2620.	5.2	334
15	Cellular Uptake of Nanoparticles by Membrane Penetration: A Study Combining Confocal Microscopy with FTIR Spectroelectrochemistry. ACS Nano, 2012, 6, 1251-1259.	7.3	313
16	Temperature: The "lgnored―Factor at the NanoBio Interface. ACS Nano, 2013, 7, 6555-6562.	7.3	299
17	Fluorescent proteins for live-cell imaging with super-resolution. Chemical Society Reviews, 2014, 43, 1088-1106.	18.7	296
18	New views on cellular uptake and trafficking of manufactured nanoparticles. Journal of the Royal Society Interface, 2013, 10, 20120939.	1.5	294

#	Article	IF	CITATIONS
19	Endo- and Exocytosis of Zwitterionic Quantum Dot Nanoparticles by Live HeLa Cells. ACS Nano, 2010, 4, 6787-6797.	7.3	279
20	Facile preparation of water-soluble fluorescent gold nanoclusters for cellular imaging applications. Nanoscale, 2011, 3, 2009.	2.8	278
21	Interleukin 21–Induced Granzyme B–Expressing B Cells Infiltrate Tumors and Regulate T Cells. Cancer Research, 2013, 73, 2468-2479.	0.4	277
22	Mg2+-dependent conformational change of RNA studied by fluorescence correlation and FRET on immobilized single molecules. Proceedings of the National Academy of Sciences of the United States of America, 2002, 99, 4284-4289.	3.3	253
23	A far-red fluorescent protein with fast maturation and reduced oligomerization tendency from Entacmaea quadricolor (Anthozoa, Actinaria). Proceedings of the National Academy of Sciences of the United States of America, 2002, 99, 11646-11651.	3.3	237
24	Neuroglobin, nitric oxide, and oxygen: Functional pathways and conformational changes. Proceedings of the National Academy of Sciences of the United States of America, 2005, 102, 8483-8488.	3.3	233
25	Fluorescent proteins for live cell imaging: Opportunities, limitations, and challenges. IUBMB Life, 2009, 61, 1029-1042.	1.5	216
26	Structural characterization of IrisFP, an optical highlighter undergoing multiple photo-induced transformations. Proceedings of the National Academy of Sciences of the United States of America, 2008, 105, 18343-18348.	3.3	211
27	Amino-Functionalized Polystyrene Nanoparticles Activate the NLRP3 Inflammasome in Human Macrophages. ACS Nano, 2011, 5, 9648-9657.	7.3	211
28	Microwave-assisted rapid synthesis of luminescent gold nanoclusters for sensing Hg2+ in living cells using fluorescence imaging. Nanoscale, 2012, 4, 4155.	2.8	211
29	Electron Transfer and Protein Dynamics in the Photosynthetic Reaction Center. Biophysical Journal, 1998, 74, 2567-2587.	0.2	204
30	Concerted action of zinc and ProSAP/Shank in synaptogenesis and synapse maturation. EMBO Journal, 2011, 30, 569-581.	3.5	204
31	mRuby, a Bright Monomeric Red Fluorescent Protein for Labeling of Subcellular Structures. PLoS ONE, 2009, 4, e4391.	1.1	197
32	Biofunctionalized, Ultrathin Coatings of Cross-Linked Star-Shaped Poly(ethylene oxide) Allow Reversible Folding of Immobilized Proteins. Journal of the American Chemical Society, 2004, 126, 4234-4239.	6.6	191
33	Quantitative analysis of the protein corona on FePt nanoparticles formed by transferrin binding. Journal of the Royal Society Interface, 2010, 7, S5-S13.	1.5	189
34	Structural basis for photo-induced protein cleavage and green-to-red conversion of fluorescent protein EosFP. Proceedings of the National Academy of Sciences of the United States of America, 2005, 102, 9156-9159.	3.3	184
35	Single-molecule Forster resonance energy transfer study of protein dynamics under denaturing conditions. Proceedings of the National Academy of Sciences of the United States of America, 2005, 102, 15471-15476.	3.3	183
36	The structure of carbonmonoxy neuroglobin reveals a heme-sliding mechanism for control of ligand affinity. Proceedings of the National Academy of Sciences of the United States of America, 2004, 101, 17351-17356.	3.3	182

#	Article	IF	CITATIONS
37	Lysosomal degradation of the carboxydextran shell of coated superparamagnetic iron oxide nanoparticles and the fate of professional phagocytes. Biomaterials, 2010, 31, 9015-9022.	5.7	173
38	The structure of murine neuroglobin: Novel pathways for ligand migration and binding. Proteins: Structure, Function and Bioinformatics, 2004, 56, 85-92.	1.5	170
39	Functionalized polystyrene nanoparticles as a platform for studying bio–nano interactions. Beilstein Journal of Nanotechnology, 2014, 5, 2403-2412.	1.5	165
40	Effect of Protein Adsorption on the Fluorescence of Ultrasmall Gold Nanoclusters. Small, 2012, 8, 661-665.	5.2	159
41	Ligand migration pathway and protein dynamics in myoglobin: A time-resolved crystallographic study on L29W MbCO. Proceedings of the National Academy of Sciences of the United States of America, 2005, 102, 11704-11709.	3.3	153
42	Zwitterionic Biocompatible Quantum Dots for Wide pH Stability and Weak Nonspecific Binding to Cells. ACS Nano, 2009, 3, 2573-2580.	7.3	153
43	Granzyme B produced by human plasmacytoid dendritic cells suppresses T-cell expansion. Blood, 2010, 115, 1156-1165.	0.6	150
44	Recent advances in synthesizing metal nanocluster-based nanocomposites for application in sensing, imaging and catalysis. Nano Today, 2019, 28, 100767.	6.2	149
45	Modeling receptor-mediated endocytosis of polymer-functionalized iron oxide nanoparticles by human macrophages. Biomaterials, 2011, 32, 547-555.	5.7	147
46	Ligand binding and protein dynamics in neuroglobin. Proceedings of the National Academy of Sciences of the United States of America, 2002, 99, 7992-7997.	3.3	145
47	Quenching of CdSeâ^'ZnS Coreâ^'Shell Quantum Dot Luminescence by Water-Soluble Thiolated Ligands. Journal of Physical Chemistry C, 2007, 111, 18589-18594.	1.5	142
48	The effect of carboxydextran-coated superparamagnetic iron oxide nanoparticles on c-Jun N-terminal kinase-mediated apoptosis in human macrophages. Biomaterials, 2010, 31, 5063-5071.	5.7	140
49	Toward a molecular understanding of nanoparticle–protein interactions. Biophysical Reviews, 2012, 4, 137-147.	1.5	139
50	In Situ Characterization of Protein Adsorption onto Nanoparticles by Fluorescence Correlation Spectroscopy. Accounts of Chemical Research, 2017, 50, 387-395.	7.6	139
51	X-ray structure determination of a metastable state of carbonmonoxy myoglobin after photodissociation Proceedings of the National Academy of Sciences of the United States of America, 1996, 93, 7013-7016.	3.3	135
52	Ligand binding to heme proteins. VI. Interconversion of taxonomic substates in carbonmonoxymyoglobin. Biophysical Journal, 1996, 71, 1563-1573.	0.2	134
53	In vitro interaction of colloidal nanoparticles with mammalian cells: What have we learned thus far?. Beilstein Journal of Nanotechnology, 2014, 5, 1477-1490.	1.5	130
54	Ultrasmall fluorescent silver nanoclusters: Protein adsorption and its effects on cellular responses. Nano Research, 2012, 5, 531-542.	5.8	129

#	Article	IF	CITATIONS
55	Motifâ€Designed Peptide Nanofibers Decorated with Graphene Quantum Dots for Simultaneous Targeting and Imaging of Tumor Cells. Advanced Functional Materials, 2015, 25, 5472-5478.	7.8	128
56	Mechanistic aspects of fluorescent gold nanocluster internalization by live HeLa cells. Nanoscale, 2013, 5, 1537.	2.8	126
57	Characterization of protein adsorption onto FePt nanoparticles using dual-focus fluorescence correlation spectroscopy. Beilstein Journal of Nanotechnology, 2011, 2, 374-383.	1.5	119
58	Photoconvertible Fluorescent Protein EosFP: Biophysical Properties and Cell Biology Applications. Photochemistry and Photobiology, 2006, 82, 351.	1.3	118
59	A photoactivatable marker protein for pulse-chase imaging with superresolution. Nature Methods, 2010, 7, 627-630.	9.0	116
60	Carbohydrate-Lectin Recognition of Sequence-Defined Heteromultivalent Glycooligomers. Journal of the American Chemical Society, 2014, 136, 2008-2016.	6.6	114
61	Spectroscopic evidence for conformational relaxation in myoglobin Proceedings of the National Academy of Sciences of the United States of America, 1992, 89, 2902-2906.	3.3	112
62	Specific Effects of Surface Amines on Polystyrene Nanoparticles in their Interactions with Mesenchymal Stem Cells. Biomacromolecules, 2010, 11, 748-753.	2.6	112
63	Ligand Binding to Heme Proteins: The Effect of Light on Ligand Binding in Myoglobin. Biochemistry, 1994, 33, 13413-13430.	1.2	111
64	Determination of rate distributions from kinetic experiments. Biophysical Journal, 1992, 61, 235-245.	0.2	110
65	Ligand binding to heme proteins: II. Transitions in the heme pocket of myoglobin. Biophysical Journal, 1993, 65, 1496-1507.	0.2	110
66	Blue light regulation of host pigment in reef-building corals. Marine Ecology - Progress Series, 2008, 364, 97-106.	0.9	110
67	Background suppression in fluorescence nanoscopy with stimulated emission double depletion. Nature Photonics, 2017, 11, 163-169.	15.6	109
68	Connection between the Taxonomic Substates and Protonation of Histidines 64 and 97 in Carbonmonoxy Myoglobin. Biophysical Journal, 1999, 77, 1036-1051.	0.2	106
69	Wnt/PCP controls spreading of Wnt/ \hat{l}^2 -catenin signals by cytonemes in vertebrates. ELife, 2018, 7, .	2.8	106
70	Single-molecule FRET Study of Denaturant Induced Unfolding of RNase H. Journal of Molecular Biology, 2006, 357, 313-324.	2.0	103
71	Photodynamics of Red Fluorescent Proteins Studied by Fluorescence Correlation Spectroscopy. Biophysical Journal, 2004, 86, 384-394.	0.2	102
72	Contributions of host and symbiont pigments to the coloration of reef corals. FEBS Journal, 2007, 274, 1102-1122.	2.2	101

#	Article	IF	CITATIONS
73	Supramolecular Self-Assembly Bioinspired Synthesis of Luminescent Gold Nanocluster-Embedded Peptide Nanofibers for Temperature Sensing and Cellular Imaging. Bioconjugate Chemistry, 2017, 28, 2224-2229.	1.8	101
74	Sensitivity Enhancement in Fluorescence Correlation Spectroscopy of Multiple Species Using Time-Gated Detection. Biophysical Journal, 2000, 79, 1129-1138.	0.2	100
75	Structural Basis of Enhanced Photoconversion Yield in Green Fluorescent Protein-like Protein Dendra2. Biochemistry, 2009, 48, 4905-4915.	1.2	100
76	SiRA: A Silicon Rhodamine-Binding Aptamer for Live-Cell Super-Resolution RNA Imaging. Journal of the American Chemical Society, 2019, 141, 7562-7571.	6.6	99
77	Specific effects of surface carboxyl groups on anionic polystyrene particles in their interactions with mesenchymal stem cells. Nanoscale, 2011, 3, 2028.	2.8	96
78	Ligand dynamics in a protein internal cavity. Proceedings of the National Academy of Sciences of the United States of America, 2003, 100, 7069-7074.	3.3	95
79	Time- and temperature dependence of large-scale conformational transitions in myoglobin. Chemical Physics, 1991, 158, 315-327.	0.9	94
80	Structural Dynamics of Myoglobin: Effect of Internal Cavities on Ligand Migration and Bindingâ€. Biochemistry, 2003, 42, 9647-9658.	1.2	94
81	Ligand binding to heme proteins: III. FTIR studies of His-E7 and Val-E11 mutants of carbonmonoxymyoglobin. Biophysical Journal, 1993, 65, 2447-2454.	0.2	92
82	Polyelectrolyte-Mediated Protein Adsorption:Â Fluorescent Protein Binding to Individual Polyelectrolyte Nanospheres. Journal of Physical Chemistry B, 2005, 109, 5418-5420.	1.2	92
83	Protein ligand migration mapped by nonequilibrium 2D-IR exchange spectroscopy. Proceedings of the National Academy of Sciences of the United States of America, 2007, 104, 14243-14248.	3.3	91
84	Fluorescent–Magnetic Hybrid Nanoparticles Induce a Doseâ€Dependent Increase in Proinflammatory Response in Lung Cells in vitro Correlated with Intracellular Localization. Small, 2010, 6, 753-762.	5.2	91
85	Small fluorescent nanoparticles at the nano–bio interface. Materials Today, 2013, 16, 58-66.	8.3	91
86	Confocal optics microscopy for biochemical and cellular high-throughput screening. Drug Discovery Today, 2003, 8, 1085-1093.	3.2	88
87	The Origin of Stark Splitting in the Initial Photoproduct State of MbCO. Journal of the American Chemical Society, 2005, 127, 40-41.	6.6	87
88	Stimulated emission depletion-based raster image correlation spectroscopy reveals biomolecular dynamics in live cells. Nature Communications, 2013, 4, 2093.	5.8	87
89	Physicochemical characterization of nanoparticles and their behavior in the biological environment. Physical Chemistry Chemical Physics, 2014, 16, 15053-15067.	1.3	87
90	Online image analysis software for photoactivation localization microscopy. Nature Methods, 2009, 6, 689-690.	9.0	86

#	Article	IF	CITATIONS
91	Biofunctionalized Polymer Surfaces Exhibiting Minimal Interaction towards Immobilized Proteins. ChemPhysChem, 2004, 5, 552-555.	1.0	84
92	Biocompatible Surfaces for Specific Tethering of Individual Protein Molecules. Journal of Physical Chemistry B, 2004, 108, 13387-13394.	1.2	84
93	The Green Fluorescent Protein: A Key Tool to Study Chemical Processes in Living Cells. Angewandte Chemie - International Edition, 2008, 47, 8992-8994.	7.2	84
94	Complex RNA Folding Kinetics Revealed by Single-Molecule FRET and Hidden Markov Models. Journal of the American Chemical Society, 2014, 136, 4534-4543.	6.6	84
95	Exploring the conformational energy landscape of proteins. Physica D: Nonlinear Phenomena, 1997, 107, 297-311.	1.3	83
96	Synthesis, patterning and applications of star-shaped poly(ethylene glycol) biofunctionalized surfaces. Molecular BioSystems, 2007, 3, 419-430.	2.9	83
97	Effects of surface functionalization on the adsorption of human serum albumin onto nanoparticles – a fluorescence correlation spectroscopy study. Beilstein Journal of Nanotechnology, 2014, 5, 2036-2047.	1.5	83
98	Live-cell imaging with EosFP and other photoactivatable marker proteins of the GFP family. Expert Review of Proteomics, 2006, 3, 361-374.	1.3	82
99	Low-threshold conical microcavity dye lasers. Applied Physics Letters, 2010, 97, .	1.5	82
100	Human B cells differentiate into granzyme Bâ€secreting cytotoxic B lymphocytes upon incomplete Tâ€cell help. Immunology and Cell Biology, 2012, 90, 457-467.	1.0	82
101	Structural Dynamics in the Active Site of Murine Neuroglobin and Its Effects on Ligand Binding. Journal of Biological Chemistry, 2004, 279, 22944-22952.	1.6	80
102	Effect of the shell on the blinking statistics of core-shell quantum dots: A single-particle fluorescence study. Physical Review B, 2007, 75, .	1.1	80
103	Gold nanoclusters as novel optical probes for in vitro and in vivo fluorescence imaging. Biophysical Reviews, 2012, 4, 313-322.	1.5	80
104	Mg2+-dependent folding of a Diels-Alderase ribozyme probed by single-molecule FRET analysis. Nucleic Acids Research, 2007, 35, 2047-2059.	6.5	79
105	A Methyl Group Controls Conformational Equilibrium in Human Mitochondrial tRNA ^{Lys} . Journal of the American Chemical Society, 2007, 129, 13382-13383.	6.6	77
106	The Nature of a Hard Protein Corona Forming on Quantum Dots Exposed to Human Blood Serum. Small, 2016, 12, 5836-5844.	5.2	77
107	Ultra-fast, high-precision image analysis for localization-based super resolution microscopy. Optics Express, 2010, 18, 11867.	1.7	76
108	Where Do We Stand with Super-Resolution Optical Microscopy?. Journal of Molecular Biology, 2016, 428, 308-322.	2.0	76

#	Article	IF	CITATIONS
109	Super-resolution RNA imaging using a rhodamine-binding aptamer with fast exchange kinetics. Nature Biotechnology, 2021, 39, 686-690.	9.4	76
110	Structure, Dynamics and Optical Properties of Fluorescent Proteins: Perspectives for Marker Development. ChemPhysChem, 2009, 10, 1369-1379.	1.0	75
111	Fast Segmentation of Stained Nuclei in Terabyte-Scale, Time Resolved 3D Microscopy Image Stacks. PLoS ONE, 2014, 9, e90036.	1.1	75
112	Comparison of Valvular Resistance, Stroke Work Loss, and Gorlin Valve Area for Quantification of Aortic Stenosis. Circulation, 1995, 91, 1196-1204.	1.6	75
113	Optimized and Far-Red-Emitting Variants of Fluorescent Protein eqFP611. Chemistry and Biology, 2008, 15, 224-233.	6.2	74
114	Pulses of Ca ²⁺ coordinate actin assembly and exocytosis for stepwise cell extension. Proceedings of the National Academy of Sciences of the United States of America, 2017, 114, 5701-5706.	3.3	74
115	Protein crystal dynamics studied by time-resolved analysis of X-ray diffuse scattering. Nature, 1989, 338, 665-666.	13.7	72
116	Ratiometric Optical Sensing of Chloride Ions with Organic Fluorophore–Gold Nanoparticle Hybrids: A Systematic Study of Design Parameters and Surface Charge Effects. Small, 2010, 6, 2590-2597.	5.2	70
117	Structural Dynamics of Myoglobin. Journal of Biological Chemistry, 2002, 277, 11636-11644.	1.6	69
118	Structural Dynamics of Myoglobin. Journal of Biological Chemistry, 2003, 278, 42532-42544.	1.6	69
119	Nanoparticles Interacting with Proteins and Cells: A Systematic Study of Protein Surface Charge Effects. Advanced Materials Interfaces, 2014, 1, 1300079.	1.9	69
120	Anthraceneâ^'BODIPY Dyads as Fluorescent Sensors for Biocatalytic Dielsâ^'Alder Reactions. Journal of the American Chemical Society, 2010, 132, 2646-2654.	6.6	67
121	Structural Basis of X-ray-Induced Transient Photobleaching in a Photoactivatable Green Fluorescent Protein. Journal of the American Chemical Society, 2009, 131, 18063-18065.	6.6	66
122	Nanoparticle interactions with live cells: Quantitative fluorescence microscopy of nanoparticle size effects. Beilstein Journal of Nanotechnology, 2014, 5, 2388-2397.	1.5	65
123	X-ray structure analysis of a metalloprotein with enhanced active-site resolution using in situ x-ray absorption near edge structure spectroscopy. Proceedings of the National Academy of Sciences of the United States of America, 2007, 104, 6211-6216.	3.3	64
124	It's cheap to be colorful. FEBS Journal, 2007, 274, 2496-2505.	2.2	64
125	Identification of GFP-like Proteins in Nonbioluminescent, Azooxanthellate Anthozoa Opens New Perspectives for Bioprospecting. Marine Biotechnology, 2004, 6, 270-7.	1.1	63
126	RITA, a novel modulator of Notch signalling, acts via nuclear export of RBP-J. EMBO Journal, 2011, 30, 43-56.	3.5	63

#	Article	IF	CITATIONS
127	Zwitterionic surface coating of quantum dots reduces protein adsorption and cellular uptake. Nanoscale, 2016, 8, 17794-17800.	2.8	63
128	Probing Electric Fields in Protein Cavities by Using the Vibrational Stark Effect of Carbon Monoxide. Biophysical Journal, 2005, 88, 1978-1990.	0.2	62
129	Data storage based on photochromic and photoconvertible fluorescent proteins. Journal of Biotechnology, 2010, 149, 289-298.	1.9	62
130	Dysferlin-mediated phosphatidylserine sorting engages macrophages in sarcolemma repair. Nature Communications, 2016, 7, 12875.	5.8	61
131	Nanoparticles for biomedical applications: exploring and exploiting molecular interactions at the nano-bio interface. Materials Today Advances, 2020, 5, 100036.	2.5	60
132	Structural Dynamics of Myoglobin:Â Spectroscopic and Structural Characterization of Ligand Docking Sites in Myoglobin Mutant L29Wâ€. Biochemistry, 2003, 42, 9633-9646.	1.2	59
133	Structural fluctuations in glass-forming liquids: Mössbauer spectroscopy on iron in glycerol. Physical Review B, 1991, 43, 3345-3350.	1.1	56
134	Red fluorescent protein eqFP611 and its genetically engineered dimeric variants. Journal of Biomedical Optics, 2005, 10, 014003.	1.4	56
135	Studying the Protein Corona on Nanoparticles by FCS. Methods in Enzymology, 2013, 519, 115-137.	0.4	55
136	Formation of a Monolayer Protein Corona around Polystyrene Nanoparticles and Implications for Nanoparticle Agglomeration. Small, 2019, 15, e1900974.	5.2	54
137	Ultrasensitive Confocal Fluorescence Microscopy of C-Reactive Protein Interacting With FcÎ ³ RIIa. Arteriosclerosis, Thrombosis, and Vascular Biology, 2004, 24, 2372-2377.	1.1	53
138	Probing Heme Protein–Ligand Interactions by UV/Visible Absorption Spectroscopy. , 2005, 305, 215-242.		52
139	Rate Processes in Proteins. Zeitschrift Fur Elektrotechnik Und Elektrochemie, 1991, 95, 272-278.	0.9	51
140	Photoconversion in the Red Fluorescent Protein from the Sea Anemone Entacmaea quadricolor: Is Cisâ^'Trans Isomerization Involved?. Journal of the American Chemical Society, 2006, 128, 6270-6271.	6.6	51
141	Structural Dynamics Controls Nitric Oxide Affinity in Nitrophorin 4. Journal of Biological Chemistry, 2004, 279, 39401-39407.	1.6	50
142	Transâ^'Cis Isomerization is Responsible for the Red-Shifted Fluorescence in Variants of the Red Fluorescent Protein eqFP611. Journal of the American Chemical Society, 2008, 130, 12578-12579.	6.6	50
143	The inability to disrupt the immunological synapse between infected human T cells and APCs distinguishes HIV-1 from most other primate lentiviruses. Journal of Clinical Investigation, 2009, 119, 2965-75.	3.9	50
144	Dual Color Photoactivation Localization Microscopy of Cardiomyopathy-associated Desmin Mutants. Journal of Biological Chemistry, 2012, 287, 16047-16057.	1.6	49

#	Article	IF	CITATIONS
145	Novel fluorescent proteins for high-content screening. Drug Discovery Today, 2006, 11, 1054-1060.	3.2	48
146	Protein structural dynamics as determined by Mössbauer spectroscopy. Hyperfine Interactions, 1988, 40, 147-157.	0.2	47
147	Myoglobin, a Paradigm in the Study of Protein Dynamics. ChemPhysChem, 2002, 3, 249.	1.0	47
148	Single-molecule FRET reveals the energy landscape of the full-length SAM-I riboswitch. Nature Chemical Biology, 2017, 13, 1172-1178.	3.9	47
149	The protein corona on nanoparticles as viewed from a nanoparticleâ€sizing perspective. Wiley Interdisciplinary Reviews: Nanomedicine and Nanobiotechnology, 2018, 10, e1500.	3.3	47
150	Light-Induced and Thermal Relaxation in a Protein. Physical Review Letters, 1995, 74, 2607-2610.	2.9	46
151	The cell end marker TeaA and the microtubule polymerase AlpA contribute to microtubule guidance at the hyphal tip cortex of <i>Aspergillus nidulans</i> for polarity maintenance. Journal of Cell Science, 2013, 126, 5400-11.	1.2	46
152	Highly Efficient One-Dimensional Triplet Exciton Transport in a Palladium–Porphyrin-Based Surface-Anchored Metal–Organic Framework. ACS Applied Materials & Interfaces, 2019, 11, 15688-15697.	4.0	46
153	RNA polymerase II clusters form in line with surface condensation on regulatory chromatin. Molecular Systems Biology, 2021, 17, e10272.	3.2	46
154	An ensemble-averaged, cell density-based digital model of zebrafish embryo development derived from light-sheet microscopy data with single-cell resolution. Scientific Reports, 2015, 5, 8601.	1.6	44
155	Molecular Switch for Sub-Diffraction Laser Lithography by Photoenol Intermediate-State Cis–Trans Isomerization. ACS Nano, 2017, 11, 6396-6403.	7.3	44
156	A simple route to highly active single-enzyme nanogels. Chemical Science, 2018, 9, 1006-1013.	3.7	44
157	Structural, dynamic, and energetic aspects of long-range electron transfer in photosynthetic reaction centers. Proceedings of the National Academy of Sciences of the United States of America, 2004, 101, 123-128.	3.3	43
158	From EosFP to mIrisFP: structureâ€based development of advanced photoactivatable marker proteins of the GFPâ€family. Journal of Biophotonics, 2011, 4, 377-390.	1.1	43
159	Ligand Migration and Protein Fluctuations in Myoglobin Mutant L29Wâ€,‡. Biochemistry, 2005, 44, 5095-5105.	1.2	41
160	Exploring Protein Structure and Dynamics under Denaturing Conditions by Single-Molecule FRET Analysis. Macromolecular Bioscience, 2006, 6, 907-922.	2.1	41
161	Rational Engineering of Photoconvertible Fluorescent Proteins for Dualâ€Color Fluorescence Nanoscopy Enabled by a Tripletâ€5tate Mechanism of Primed Conversion. Angewandte Chemie - International Edition, 2017, 56, 11628-11633.	7.2	41
162	Chromophore-Protein Interactions in the Anthozoan Green Fluorescent Protein asFP499. Biophysical Journal, 2006, 91, 4210-4220.	0.2	40

#	Article	IF	CITATIONS
163	Mediation of a non-proteolytic activation of complement component C3 by phospholipid vesicles. Biomaterials, 2014, 35, 3688-3696.	5.7	40
164	Superresolution and pulse-chase imaging reveal the role of vesicle transport in polar growth of fungal cells. Science Advances, 2018, 4, e1701798.	4.7	40
165	Conformational substates in azurin Proceedings of the National Academy of Sciences of the United States of America, 1992, 89, 9681-9685.	3.3	39
166	Searching for Neuroglobin's role in the brain. IUBMB Life, 2007, 59, 490-497.	1.5	39
167	Reversible Reconfiguration of DNA Origami Nanochambers Monitored by Singleâ€Molecule FRET. Angewandte Chemie - International Edition, 2015, 54, 3592-3597.	7.2	39
168	Super-resolution imaging-based single particle tracking reveals dynamics of nanoparticle internalization by live cells. Nanoscale, 2016, 8, 7423-7429.	2.8	39
169	Simulation of FRET dyes allows quantitative comparison against experimental data. Journal of Chemical Physics, 2018, 148, 123321.	1.2	39
170	Thr-E11 Regulates O2 Affinity in Cerebratulus lacteus Mini-hemoglobin. Journal of Biological Chemistry, 2004, 279, 33662-33672.	1.6	38
171	Conformational Heterogeneity in RNA Polymerase Observed by Single-Pair FRET Microscopy. Biophysical Journal, 2006, 90, 4605-4617.	0.2	38
172	Spectroscopic Study of Substrate Binding to the Carbonmonoxy Form of Dehaloperoxidase fromAmphitriteornata. Journal of Physical Chemistry B, 2006, 110, 13264-13276.	1.2	38
173	Superresolution microscopy reveals a dynamic picture of cell polarity maintenance during directional growth. Science Advances, 2015, 1, e1500947.	4.7	38
174	Sculpting an RNA Conformational Energy Landscape by a Methyl Group Modification—A Singleâ€Molecule FRET Study. Angewandte Chemie - International Edition, 2008, 47, 4326-4330.	7.2	37
175	Structural Dynamics of Myoglobin:  FTIR-TDS Study of NO Migration and Bindingâ€. Biochemistry, 2008, 47, 935-948.	1.2	37
176	Charge Recombination and Protein Dynamics in Bacterial Photosynthetic Reaction Centers Entrapped in a Sol-Gel Matrix. Biophysical Journal, 2003, 85, 1851-1870.	0.2	36
177	Two-Photon Excitation and Photoconversion of EosFP in Dual-Color 4Pi Confocal Microscopy. Biophysical Journal, 2007, 92, 4451-4457.	0.2	36
178	Photoconversion of the Fluorescent Protein EosFP: A Hybrid Potential Simulation Study Reveals Intersystem Crossings. Journal of the American Chemical Society, 2009, 131, 16814-16823.	6.6	36
179	Dynamics of Actin Cables in Polarized Growth of the Filamentous Fungus Aspergillus nidulans. Frontiers in Microbiology, 2016, 7, 682.	1.5	36
180	Protein-based fluorescent nanoparticles for super-resolution STED imaging of live cells. Chemical Science, 2017, 8, 2396-2400.	3.7	36

#	Article	IF	CITATIONS
181	CD Spectroscopy: An Essential Tool for Quality Control of Protein Folding. Methods in Molecular Biology, 2015, 1261, 255-276.	0.4	36
182	The Effect of Ligand Dynamics on Heme Electronic Transition Band III in Myoglobin. Biophysical Journal, 2002, 82, 1059-1067.	0.2	35
183	Ligand Migration and Binding in the Dimeric Hemoglobin of <i>Scapharca inaequivalvis</i> [,] . Biochemistry, 2007, 46, 14018-14031.	1.2	35
184	Fast and Efficient Molecule Detection in Localization-Based Super-Resolution Microscopy by Parallel Adaptive Histogram Equalization. ACS Nano, 2013, 7, 5207-5214.	7.3	35
185	Monomeric Garnet, a far-red fluorescent protein for live-cell STED imaging. Scientific Reports, 2015, 5, 18006.	1.6	35
186	Precise background subtraction in stimulated emission double depletion nanoscopy. Optics Letters, 2017, 42, 831.	1.7	35
187	Ligand Migration between Internal Docking Sites in Photodissociated Carbonmonoxy Neuroglobin. Journal of Physical Chemistry B, 2009, 113, 15334-15343.	1.2	33
188	Organization of perinuclear actin in live tobacco cells observed by PALM with optical sectioning. Journal of Plant Physiology, 2014, 171, 97-108.	1.6	33
189	EmbryoMiner: A new framework for interactive knowledge discovery in large-scale cell tracking data of developing embryos. PLoS Computational Biology, 2018, 14, e1006128.	1.5	33
190	Circular Dichroism Spectroscopy for the Study of Protein–Ligand Interactions. , 2005, 305, 343-364.		32
191	A Green Fluorescent Protein with Photoswitchable Emission from the Deep Sea. PLoS ONE, 2008, 3, e3766.	1.1	32
192	A far-red emitting fluorescent marker protein, mGarnet2, for microscopy and STED nanoscopy. Chemical Communications, 2017, 53, 979-982.	2.2	32
193	Development of Bag-1L as a therapeutic target in androgen receptor-dependent prostate cancer. ELife, 2017, 6, .	2.8	32
194	Light-Induced Relaxation of Photolyzed Carbonmonoxy Myoglobin: A Temperature-Dependent X-Ray Absorption Near-Edge Structure (XANES) Study. Biophysical Journal, 2005, 88, 2954-2964.	0.2	31
195	Exploring Chromophoreâ^'Protein Interactions in Fluorescent Protein cmFP512 fromCerianthus membranaceus: X-ray Structure Analysis and Optical Spectroscopyâ€. Biochemistry, 2006, 45, 12942-12953.	1.2	31
196	Câ€reactive protein specifically binds to Fcγ receptor type I on a macrophageâ€like cell line. European Journal of Immunology, 2008, 38, 1414-1422.	1.6	31
197	The Apolar Channel in Cerebratulus lacteus Hemoglobin Is the Route for O2 Entry and Exit. Journal of Biological Chemistry, 2008, 283, 35689-35702.	1.6	31
198	Localization and Dynamics of Glucocorticoid Receptor at the Plasma Membrane of Activated Mast Cells. Small, 2014, 10, 1991-1998.	5.2	31

#	Article	IF	CITATIONS
199	Towards a molecular-level understanding of the protein corona around nanoparticles – Recent advances and persisting challenges. Current Opinion in Biomedical Engineering, 2019, 10, 11-22.	1.8	31
200	Targeted Green-Red Photoconversion of EosFP, a Fluorescent Marker Protein. Journal of Biological Physics, 2005, 31, 249-259.	0.7	30
201	An integrated instrumental setup for the combination of atomic force microscopy with optical spectroscopy. Biopolymers, 2006, 82, 410-414.	1.2	30
202	Mechanistic Insights into Reversible Photoactivation in Proteins of the GFP Family. Biophysical Journal, 2012, 103, 2521-2531.	0.2	30
203	Structural factors controlling ligand binding to myoglobin: A kinetic hole-burning study. Proceedings of the National Academy of Sciences of the United States of America, 1998, 95, 6762-6767.	3.3	29
204	Determinants of Substrate Internalization in the Distal Pocket of Dehaloperoxidase Hemoglobin of <i>Amphitrite ornata</i> . Biochemistry, 2008, 47, 12985-12994.	1.2	29
205	Pax6 organizes the anterior eye segment by guiding two distinct neural crest waves. PLoS Genetics, 2020, 16, e1008774.	1.5	29
206	Photodissociation and Rebinding of H2O to Ferrous Sperm Whale Myoglobin. Journal of the American Chemical Society, 1998, 120, 2981-2982.	6.6	28
207	Dual-color dual-focus line-scanning FCS for quantitative analysis of receptor-ligand interactions in living specimens. Scientific Reports, 2015, 5, 10149.	1.6	28
208	In Situ Monitoring of the Intracellular Stability of Nanoparticles by Using Fluorescence Lifetime Imaging. Small, 2016, 12, 868-873.	5.2	28
209	Crystallization and preliminary X-ray diffraction analysis of the red fluorescent protein eqFP611. Acta Crystallographica Section D: Biological Crystallography, 2003, 59, 1253-1255.	2.5	27
210	Endothelin Receptor in Virus-Like Particles:Â Ligand Binding Observed by Fluorescence Fluctuation Spectroscopyâ€. Biochemistry, 2004, 43, 9021-9028.	1.2	27
211	Automated High Content Screening for Phosphoinositide 3 Kinase Inhibition Using an AKT1 Redistribution Assay. Combinatorial Chemistry and High Throughput Screening, 2006, 9, 339-350.	0.6	27
212	Optical imaging of nanoscale cellular structures. Biophysical Reviews, 2010, 2, 147-158.	1.5	27
213	Temperature Dependence of the Heat Diffusivity of Proteins. Journal of Physical Chemistry A, 2012, 116, 2620-2628.	1.1	27
214	Low affinity binding of plasma proteins to lipid-coated quantum dots as observed by in situ fluorescence correlation spectroscopy. Nanoscale, 2015, 7, 9980-9984.	2.8	27
215	Measuring ligand-cell surface receptor affinities with axial line-scanning fluorescence correlation spectroscopy. ELife, 2020, 9, .	2.8	27
216	Mössbauer studies of bound diffusion in a model polymer system. Physical Review B, 1992, 45, 7716-7723.	1.1	26

#	Article	IF	CITATIONS
217	Structural Heterogeneity and Ligand Binding in Carbonmonoxy Myoglobin Crystals at Cryogenic Temperatures. Biochemistry, 1998, 37, 6819-6823.	1.2	26
218	Analysis of Ligand Binding to Heme Proteins Using a Fluctuating Path Description. The Journal of Physical Chemistry, 1995, 99, 9278-9282.	2.9	25
219	Infrared Study of Carbon Monoxide Migration among Internal Cavities of Myoglobin Mutant L29W. Journal of Biological Physics, 2002, 28, 163-172.	0.7	25
220	Single-Molecule FRET Reveals a Cooperative Effect of Two Methyl Group Modifications in the Folding of Human Mitochondrial tRNALys. Chemistry and Biology, 2011, 18, 928-936.	6.2	25
221	NMR Studies of Protein–Ligand Interactions. Methods in Molecular Biology, 2012, 831, 233-259.	0.4	25
222	Dynamics of protein-water systems revealed by Rayleigh scattering of Mössbauer radiation (RSMR). Hyperfine Interactions, 1990, 53, 59-73.	0.2	24
223	Metal nanoclusters: Protein corona formation and implications for biological applications. International Journal of Biochemistry and Cell Biology, 2016, 75, 175-179.	1.2	23
224	Total internal reflection fluorescence microscopy—a powerful tool to study single quantum dots. Applied Surface Science, 2004, 234, 86-92.	3.1	22
225	Evidence of a Folding Intermediate in RNase H from Singleâ€Molecule FRET Experiments. ChemPhysChem, 2011, 12, 627-633.	1.0	22
226	FTIR Study of Conformational Substates in the CO Adduct of CytochromecOxidase fromRhodobacter sphaeroidesâ€. Biochemistry, 1996, 35, 16782-16788.	1.2	21
227	Affinity of C-Reactive Protein toward FcγRI Is Strongly Enhanced by the γ-Chain. American Journal of Pathology, 2007, 170, 755-763.	1.9	21
228	Ligand Dynamics in Heme Proteins Observed by Fourier Transform Infrared Spectroscopy at Cryogenic Temperatures. Methods in Enzymology, 2008, 437, 347-378.	0.4	21
229	Chromophore photophysics and dynamics in fluorescent proteins of the GFP family. Journal of Physics Condensed Matter, 2016, 28, 443001.	0.7	21
230	Confocal laser scanning microscopy with spatiotemporal structured illumination. Optics Letters, 2016, 41, 1193.	1.7	21
231	Self-assembled thermosensitive luminescent nanoparticles with peptide-Au conjugates for cellular imaging and drug delivery. Chinese Chemical Letters, 2020, 31, 859-864.	4.8	21
232	Glass-like behaviour of proteins as seen by Mössbauer spectroscopy. Journal of Non-Crystalline Solids, 1991, 131-133, 362-368.	1.5	20
233	Ligand binding to heme proteins. V. Light-induced relaxation in proximal mutants L89I and H97F of carbonmonoxymyoglobin. Biophysical Journal, 1995, 68, 2497-2504.	0.2	20
234	Confocal Fluorescence Microscopy for High-Throughput Screening of G-Protein Coupled Receptors. Current Medicinal Chemistry, 2005, 12, 2551-2559.	1.2	20

#	Article	IF	CITATIONS
235	Restricted rotational motion of CO in a protein internal cavity: Evidence for nonseparating correlation functions from IR pump-probe spectroscopy. Journal of Chemical Physics, 2005, 122, 124505.	1.2	20
236	Fluctuation correlation spectroscopy for the advanced physics laboratory. American Journal of Physics, 2005, 73, 1129-1134.	0.3	20
237	Ligand and Substrate Migration in Human Indoleamine 2,3-Dioxygenase. Journal of Biological Chemistry, 2009, 284, 31548-31554.	1.6	20
238	Live Imaging of Xwnt5A-ROR2 Complexes. PLoS ONE, 2014, 9, e109428.	1.1	20
239	Super-resolution localization microscopy with photoactivatable fluorescent marker proteins. Protoplasma, 2014, 251, 349-362.	1.0	20
240	Genetic evidence for a microtubule-capture mechanism during polar growth of <i>Aspergillus nidulans</i> . Journal of Cell Science, 2015, 128, 3569-82.	1.2	20
241	Photoswitchable Fluorescent Proteins: Do Not Always Look on the Bright Side. ACS Nano, 2016, 10, 9104-9108.	7.3	20
242	Single-molecule Förster resonance energy transfer studies of RNA structure, dynamics and function. Biophysical Reviews, 2009, 1, 161-176.	1.5	19
243	Ligand Migration and Binding in Nonsymbiotic Hemoglobins of <i>Arabidopsis thaliana</i> . Biochemistry, 2010, 49, 7448-7458.	1.2	19
244	Substrate Inhibition in Human Indoleamine 2,3-Dioxygenase. Journal of Physical Chemistry Letters, 2014, 5, 756-761.	2.1	19
245	Hematopoietic and mesenchymal stem cells: polymeric nanoparticle uptake and lineage differentiation. Beilstein Journal of Nanotechnology, 2015, 6, 383-395.	1.5	19
246	Rac-mediated Stimulation of Phospholipase Cγ2 Amplifies B Cell Receptor-induced Calcium Signaling. Journal of Biological Chemistry, 2015, 290, 17056-17072.	1.6	19
247	Nanoparticle Probes for Superâ€Resolution Fluorescence Microscopy. ChemNanoMat, 2018, 4, 253-264.	1.5	19
248	Structural Identification of Spectroscopic Substates in Neuroglobin. ChemPhysChem, 2010, 11, 119-129.	1.0	18
249	Ligand dynamics in heme proteins observed by Fourier transform infrared-temperature derivative spectroscopy. Biochimica Et Biophysica Acta - Proteins and Proteomics, 2011, 1814, 1030-1041.	1.1	18
250	Cytoplasmic Transport Machinery of the SPF27 Homologue Num1 in Ustilago maydis. Scientific Reports, 2018, 8, 3611.	1.6	18
251	Steric constraints in the retinal binding pocket of sensory rhodopsin I. Biochemistry, 1993, 32, 10224-10232.	1.2	17
252	Acceleration of tissue phase mapping by k-t BLAST: a detailed analysis of the influence of k-t-BLAST for the quantification of myocardial motion at 3T. Journal of Cardiovascular Magnetic Resonance, 2011, 13, 5.	1.6	17

#	Article	IF	CITATIONS
253	Oneâ€&tep Fabrication of Perovskiteâ€Based Upconversion Devices. ChemPhotoChem, 2020, 4, 704-712.	1.5	17
254	Angular dependent rayleigh scattering of Mössbauer radiation on proteins. Hyperfine Interactions, 1989, 47-48, 299-310.	0.2	16
255	Structural dynamics of myoglobin: an infrared kinetic study of ligand migration in mutants YQR and YQRF. Biophysical Chemistry, 2004, 109, 41-58.	1.5	16
256	RNA Intramolecular Dynamics by Singleâ€Molecule FRET. Current Protocols in Nucleic Acid Chemistry, 2008, 34, Unit 11.12.	0.5	16
257	Three critical hydrogen bonds determine the catalytic activity of the Diels–Alderase ribozyme. Nucleic Acids Research, 2012, 40, 1318-1330.	6.5	16
258	Dual-mode phase and fluorescence imaging with a confocal laser scanning microscope. Optics Letters, 2018, 43, 5689.	1.7	16
259	Influence of Distal Residue B10 on CO Dynamics in Myoglobin and Neuroglobin. Journal of Biological Physics, 2007, 33, 357-370.	0.7	15
260	Cell-Based Assays in Practice: Cell Markers from Autofluorescent Proteins of the GFP-Family. Combinatorial Chemistry and High Throughput Screening, 2008, 11, 602-609.	0.6	15
261	Exploring color tuning strategies in red fluorescent proteins. Photochemical and Photobiological Sciences, 2015, 14, 200-212.	1.6	15
262	Research Update: Interfacing ultrasmall metal nanoclusters with biological systems. APL Materials, 2017, 5, 053101.	2.2	15
263	Wavelet-based background and noise subtraction for fluorescence microscopy images. Biomedical Optics Express, 2021, 12, 969.	1.5	15
264	Single-Molecule Fluorescence Studies of Protein Folding. Methods in Molecular Biology, 2009, 490, 311-337.	0.4	15
265	Rayleigh scattering of Mössbauer radiation on met-myoglobin. Hyperfine Interactions, 1986, 29, 1451-1454.	0.2	14
266	The similarity in the dynamics of myoglobin and glycerol as seen from Mössbauer spectroscopy on 57Fe. Journal of Molecular Liquids, 1989, 42, 145-153.	2.3	14
267	Ligand Binding and Protein Dynamics in Cupredoxins. Biochemistry, 1995, 34, 12170-12177.	1.2	14
268	Genetically encodable fluorescent protein markers in advanced optical imaging. Methods and Applications in Fluorescence, 2022, 10, 042002.	1.1	14
269	Pressure effects on the dark-adaptation of bacteriorhodopsin. Biophysical Journal, 1993, 64, 1187-1193.	0.2	13
270	A Fatigueâ€Resistant Photoswitchable Fluorescent Protein for Optical Nanoscopy. Angewandte Chemie - International Edition, 2012, 51, 1312-1314.	7.2	13

#	Article	IF	CITATIONS
271	Reactionâ€Pathway Selection in the Structural Dynamics of a Heme Protein. Chemistry - A European Journal, 2013, 19, 3558-3562.	1.7	13
272	Assessment of in vitro particle dosimetry models at the single cell and particle level by scanning electron microscopy. Journal of Nanobiotechnology, 2018, 16, 100.	4.2	13
273	Fluorescent proteins of the EosFP clade: intriguing marker tools with multiple photoactivation modes for advanced microscopy. RSC Chemical Biology, 2021, 2, 796-814.	2.0	13
274	The Mössbauer effect and collective motions in glass-forming liquids and polymeric networks. Hyperfine Interactions, 1994, 90, 243-264.	0.2	12
275	Evaluation of Genetically Encoded Chemical Tags as Orthogonal Fluorophore Labeling Tools for Single-Molecule FRET Applications. Journal of Physical Chemistry B, 2015, 119, 6611-6619.	1.2	12
276	Generating semi-synthetic validation benchmarks for embryomics. , 2016, , .		12
277	Efficiency of bulk perovskite-sensitized upconversion: Illuminating matters. Applied Physics Letters, 2021, 118, .	1.5	12
278	Protein adsorption onto nanomaterials engineered for theranostic applications. Nanotechnology, 2022, 33, 262001.	1.3	12
279	Simple model of the diffusive scattering law in glass-forming liquids. Physical Review B, 1994, 49, 15607-15614.	1.1	11
280	Transient ligand docking sites in Cerebratulus lacteus mini-hemoglobin. Gene, 2007, 398, 208-223.	1.0	11
281	Axial Resolution Enhancement by 4Pi Confocal Fluorescence Microscopy with Two-Photon Excitation. Journal of Biological Physics, 2007, 33, 433-443.	0.7	11
282	High Content Screening of CXCR2-Dependent Signalling Pathways. Combinatorial Chemistry and High Throughput Screening, 2010, 13, 3-15.	0.6	11
283	Single-Molecule FRET Studies of Counterion Effects on the Free Energy Landscape of Human Mitochondrial Lysine tRNA. Biochemistry, 2011, 50, 3107-3115.	1.2	11
284	Antiviral Vaccines License T Cell Responses by Suppressing Granzyme B Levels in Human Plasmacytoid Dendritic Cells. Journal of Immunology, 2013, 191, 1144-1153.	0.4	11
285	Substrate binding in human indoleamine 2,3-dioxygenase 1: A spectroscopic analysis. Biochimica Et Biophysica Acta - Proteins and Proteomics, 2017, 1865, 453-463.	1.1	11
286	Refractive index measurement of suspended cells using opposed-view digital holographic microscopy. Applied Optics, 2017, 56, 9000.	0.9	11
287	FTIR Study of ATP-Induced Changes in Na+/K+-ATPase from Duck Supraorbital Glands. Biophysical Journal, 2003, 85, 3707-3717.	0.2	10
288	Nerve Globins in Invertebrates. IUBMB Life, 2004, 56, 653-656.	1.5	10

#	Article	IF	CITATIONS
289	A Spectroscopic Study of Structural Heterogeneity and Carbon Monoxide Binding in Neuroglobin. Journal of Biological Physics, 2005, 31, 417-432.	0.7	10
290	Cardiac phase-specific shimming (CPSS) for SSFP MR cine imaging at 3 T. Physics in Medicine and Biology, 2009, 54, N467-N478.	1.6	10
291	Volumetric motion quantification by 3D tissue phase mapped CMR. Journal of Cardiovascular Magnetic Resonance, 2012, 14, 73.	1.6	10
292	The multi-state energy landscape of the SAM-I riboswitch: A single-molecule Förster resonance energy transfer spectroscopy study. Journal of Chemical Physics, 2018, 148, 123324.	1.2	10
293	Different Mechanisms of Catalytic Complex Formation in Two L-Tryptophan Processing Dioxygenases. Frontiers in Molecular Biosciences, 2017, 4, 94.	1.6	10
294	Relaxation and Disorder in Proteins. , 1994, , 591-614.		10
295	Temperature dependence of the dynamics of ultrafine particles in a polymeric network. Hyperfine Interactions, 1990, 56, 1471-1476.	0.2	9
296	Quantum-mechanical tunneling of water in heme proteins. Journal of Physical Organic Chemistry, 2000, 13, 659-663.	0.9	9
297	The "Wiggling and Jiggling of Atoms―Leading to Excitedâ€State Proton Transfer in Green Fluorescent Protein. ChemPhysChem, 2010, 11, 971-974.	1.0	9
298	Fast Folding Dynamics of an Intermediate State in RNase H Measured by Single-Molecule FRET. Journal of Physical Chemistry B, 2016, 120, 641-649.	1.2	9
299	Distinct amino acid motifs carrying multiple positive charges regulate membrane targeting of dysferlin and MG53. PLoS ONE, 2018, 13, e0202052.	1.1	9
300	Super-resolution imaging of densely packed DNA in nuclei of zebrafish embryos using stimulated emission double depletion microscopy. Journal Physics D: Applied Physics, 2019, 52, 414001.	1.3	9
301	Determining chemical rate coefficients using time-gated fluorescence correlation spectroscopy. Journal of Physical Organic Chemistry, 2000, 13, 654-658.	0.9	8
302	Acceleration of tissue phase mapping with sensitivity encoding at 3T. Journal of Cardiovascular Magnetic Resonance, 2011, 13, 59.	1.6	8
303	A combined single-molecule FRET and tryptophan fluorescence study of RNase H folding under acidic conditions. Chemical Physics, 2012, 396, 3-9.	0.9	8
304	Single-Molecule FRET Studies of RNA Folding: A Diels–Alderase Ribozyme with Photolabile Nucleotide Modifications. Journal of Physical Chemistry B, 2013, 117, 12800-12806.	1.2	8
305	Photoactivatable Fluorescent Proteins for Super-resolution Microscopy. Methods in Molecular Biology, 2014, 1148, 239-260.	0.4	8
306	Effect of Protein Adsorption on the Fluorescence of Ultrasmall Gold Nanoclusters. Small, 2014, 10, 1667-1667.	5.2	8

#	Article	IF	CITATIONS
307	Fourier transform infrared spectroscopy study ofÂligand photodissociation and migration in in in in in in in in	0.8	8
308	A multiwire proportional counter with spherical drift chamber for protein crystallography with X-rays and gamma-rays. Nuclear Instruments and Methods in Physics Research, Section A: Accelerators, Spectrometers, Detectors and Associated Equipment, 1987, 256, 581-586.	0.7	7
309	The role of entropy in the discrimination between CO and O 2 in myoglobin. European Biophysics Journal, 1997, 26, 209-214.	1.2	7
310	Molecular dynamics simulation of the acidic compact state of apomyoglobin from yellowfin tuna. Proteins: Structure, Function and Bioinformatics, 2009, 74, 273-290.	1.5	7
311	SAR reduced black-blood cine TPM for increased temporal resolution at 3T. Magnetic Resonance Materials in Physics, Biology, and Medicine, 2011, 24, 127-135.	1.1	7
312	Ligand migration in human indoleamineâ \in 2,3 dioxygenase. IUBMB Life, 2011, 63, 153-159.	1.5	7
313	Surface energy of phospholipid bilayers and the correlation to their hydration. Journal of Colloid and Interface Science, 2013, 390, 267-274.	5.0	7
314	Nanocrystals by design. Nature Chemistry, 2015, 7, 769-770.	6.6	7
315	Pulsed interleaved excitation-based line-scanning spatial correlation spectroscopy (PIE-lsSCS). Scientific Reports, 2018, 8, 16722.	1.6	7
316	MondoA regulates gene expression in cholesterol biosynthesis-associated pathways required for zebrafish epiboly. ELife, 2020, 9, .	2.8	7
317	Rayleigh scattering of Mössbauer radiation on a myoglobin single crystal. Hyperfine Interactions, 1992, 71, 1319-1322.	0.2	6
318	Ligand Binding With Stopped-Flow Rapid Mixing. , 2005, 305, 323-342.		6
319	CXCR2 Inverse Agonism Detected by Arrestin Redistribution. Journal of Biomolecular Screening, 2009, 14, 1076-1091.	2.6	6
320	Facile synthesis of fluorescent gold nanoclusters and their application in cellular imaging. Proceedings of SPIE, 2012, , .	0.8	6
321	Attachment of Proteins to Surfaces by Fluorous–Fluorous Interactions Restoring Their Structure and Activity. ChemPlusChem, 2012, 77, 1066-1070.	1.3	6
322	Rational Engineering of Photoconvertible Fluorescent Proteins for Dualâ€Color Fluorescence Nanoscopy Enabled by a Tripletâ€State Mechanism of Primed Conversion. Angewandte Chemie, 2017, 129, 11786-11791.	1.6	6
323	Lef1 regulates caveolin expression and caveolin dependent endocytosis, a process necessary for Wnt5a/Ror2 signaling during Xenopus gastrulation. Scientific Reports, 2019, 9, 15645.	1.6	6
324	Structural heterogeneity in proteins at cryogenic temperatures. Cooling rate dependence. Chemical Physics Letters, 1993, 216, 275-280.	1.2	5

#	Article	IF	CITATIONS
325	Heme geometry in the 10 K photoproduct from sperm whale carbonmonoxymyoglobin. Biophysical Chemistry, 1996, 60, 111-117.	1.5	5
326	Ligand Binding to Heme Proteins: A Comparison of Cytochrome c Variants with Globins. Journal of Physical Chemistry B, 2012, 116, 12180-12188.	1.2	5
327	InÂvivo labeling of peroxisomes by photoconvertible mEos2 in myelinating glia of mice. Biochimie, 2014, 98, 127-134.	1.3	5
328	Comparison of ligand migration and binding in heme proteins of the globin family. Chinese Physics B, 2015, 24, 128705.	0.7	5
329	Fourier transform infrared spectroscopy study ofÂligand photodissociation and migration in in in inducible nitric oxide synthase. F1000Research, 2014, 3, 290.	0.8	5
330	Brownian motion-based nanoparticle sizing—A powerful approach for <i>in situ</i> analysis of nanoparticle-protein interactions. Biointerphases, 2020, 15, 061201.	0.6	5
331	A chemical probe for BAG1 targets androgen receptor-positive prostate cancer through oxidative stress signaling pathway. IScience, 2022, 25, 104175.	1.9	5
332	High-Throughput Screening of Interactions Between G Protein-Coupled Receptors and Ligands Using Confocal Optics Microscopy. , 2005, 305, 365-384.		4
333	EXPLORING THE FOLDING FREE ENERGY LANDSCAPE OF SMALL RNA MOLECULES BY SINGLE-PAIR FÖRSTER RESONANCE ENERGY TRANSFER. Biophysical Reviews and Letters, 2008, 03, 439-457.	0.9	4
334	Nanoparticle Interaction with Plasma Proteins as It Relates to Biodistribution. Frontiers in Nanobiomedical Research, 2013, , 151-172.	0.1	4
335	Substrate Binding Primes Human Tryptophan 2,3-Dioxygenase for Ligand Binding. Journal of Physical Chemistry B, 2017, 121, 7412-7420.	1.2	4
336	"siRNA traffic lights― arabino-configured 2′-anchors for fluorescent dyes are key for dual color readout in cell imaging. Organic and Biomolecular Chemistry, 2018, 16, 3726-3731.	1.5	4
337	Structural Fluctuations in Myoglobin. Springer Series in Biophysics, 1987, , 30-33.	0.4	4
338	Exploring the energy landscape of a SAM-I riboswitch. Journal of Biological Physics, 2021, 47, 371-386.	0.7	4
339	The effect of protein internal cavities on ligand migration and binding in myoglobin. Micron, 2004, 35, 67-69.	1.1	3
340	Ultrasensitive Fluorescence Microscopy Studies of Protein Interactions with Functionalized Surfaces. Zeitschrift Fur Physikalische Chemie, 2007, 221, 75-93.	1.4	3
341	Probes for Nanoscopy: Fluorescent Proteins. Springer Series on Fluorescence, 2011, , 111-158.	0.8	3
342	Time-Lapse Super-Resolution Imaging of Apical Membrane Protein Domains in Live Filamentous Fungi. Biophysical Journal, 2013, 104, 652a.	0.2	3

#	Article	IF	CITATIONS
343	Lipid membranes and single ion channel recording for the advanced physics laboratory. American Journal of Physics, 2014, 82, 502-509.	0.3	3
344	Impact of Transition Metal Doping on the Structural and Optical Properties of Halide Perovskites. Chemistry of Materials, 2021, 33, 6099-6107.	3.2	3
345	Allele-specific endogenous tagging and quantitative analysis of β-catenin in colorectal cancer cells. ELife, 2022, 11, .	2.8	3
346	Single molecule localization-based analysis of clathrin-coated pit and caveolar dynamics. Nanoscale Horizons, 2022, 7, 385-395.	4.1	3
347	Homodimerization Counteracts the Detrimental Effect of Nitrogenous Heme Ligands on the Enzymatic Activity of <i>Acanthamoeba castellanii</i> CYP51. Biochemistry, 2022, 61, 1363-1377.	1.2	3
348	Mössbauer investigations on glass-forming organic liquids. Hyperfine Interactions, 1992, 70, 1125-1128.	0.2	2
349	Structural heterogeneity in proteins at cryogenic temperatures. Cooling rate dependence. Chemical Physics Letters, 1994, 221, 188.	1.2	2
350	Photoactivation in green to red converting EosFP and other fluorescent proteins from the GFP family. , 2006, , .		2
351	Structure–Function Relationships in Fluorescent Marker Proteins of the Green Fluorescent Protein Family. Springer Series on Fluorescence, 2011, , 241-263.	0.8	2
352	Fluorescent Proteins: Nature's Colorful Gifts for Live Cell Imaging. Springer Series on Fluorescence, 2011, , 3-33.	0.8	2
353	Combination of tagging and tissue phase mapping to accelerate myocardial motion measurements in three directions. Magnetic Resonance Materials in Physics, Biology, and Medicine, 2013, 26, 239-247.	1.1	2
354	Fluorescent nanoparticle interactions with biological systems: What have we learned so far?. , 2015, , .		2
355	Kinetic Study of Ligand Binding and Conformational Changes in Inducible Nitric Oxide Synthase. Journal of Physical Chemistry B, 2018, 122, 11048-11057.	1.2	2
356	Superresolution Imaging of Live Cells with Genetically Encoded Silicon Rhodamine-Binding RNA Aptamers. Biophysical Journal, 2020, 118, 145a.	0.2	2
357	Fluorescence Lifetime Imaging Microscopy (FLIM) of Intracellular Transport by Means of Doubly Labelled siRNA Architectures. ChemBioChem, 2021, 22, 2561-2567.	1.3	2
358	C-Reactive Protein and Atherosclerosis: An Update. Vascular Disease Prevention, 2008, 5, 178-182.	0.2	2
359	Aminoâ€functionalized polystyrene nanoparticles activate the NLRP3 inflammasome in human macrophages. FASEB Journal, 2013, 27, 575.6.	0.2	2
360	Two plus one is almost three: A fast approximation for multi-view deconvolution. Biomedical Optics Express, 2022, 13, 147-158.	1.5	2

#	Article	IF	CITATIONS
361	Interaction between ATP and the Na/Kâ€ATPase from Duck Supraorbital Salt Glands. Annals of the New York Academy of Sciences, 2003, 986, 293-295.	1.8	1
362	Dimeric variants of the red fluorescent protein eqFP611 generated by site-directed mutagenesis. , 2004, 5329, 23.		1
363	Lasing in dye-doped high-Q conical polymeric microcavities. , 2011, , .		1
364	Colocalization Analysis of Mutant and Wildtype Desmin using Dual Color Super-Resolution Microscopy. Biophysical Journal, 2012, 102, 722a.	0.2	1
365	Fluorescent Proteins from the Oceans: Marine Macromolecules as Advanced Imaging Tools for Biomedical Research. , 2012, , 1231-1257.		1
366	An engineered heme–copper center in myoglobin: CO migration and binding. Biochimica Et Biophysica Acta - Proteins and Proteomics, 2013, 1834, 1824-1831.	1.1	1
367	Unravelling RNA–Substrate Interactions in a Ribozymeâ€Catalysed Reaction Using Fluorescent Turnâ€On Probes. Chemistry - A European Journal, 2015, 21, 5864-5871.	1.7	1
368	Automation strategies for large-scale 3D image analysis. Automatisierungstechnik, 2016, 64, 555-566.	0.4	1
369	Localization Microscopy. PhotonicsViews, 2020, 17, 27-31.	0.1	1
370	Protein Adsorption Onto Polystyrene Nanoparticles and its Effect on Nanoparticle Agglomeration. Biophysical Journal, 2020, 118, 625a.	0.2	1
371	Axial line-scanning stimulated emission depletion fluorescence correlation spectroscopy. Optics Letters, 2021, 46, 2184.	1.7	1
372	Ecotoxicological Aspects of Nanomaterials in the Aquatic Environment. , 2016, , 151-172.		1
373	Sub-Wavelength Optical Fluorescence Microscopy for Biological Applications. NATO Science for Peace and Security Series B: Physics and Biophysics, 2013, , 47-71.	0.2	1
374	Aminoâ€functionalized nanoparticles inhibit mTOR and induce cell cycle arrest and apoptosis in leukemia cells. FASEB Journal, 2013, 27, 575.7.	0.2	1
375	Genetic evidence for a microtubule-capture mechanism during polarised growth of <i>Aspergillus nidulans</i> . Development (Cambridge), 2015, 142, e1.2-e1.2.	1.2	1
376	Confocal and Super-resolution Imaging of RNA in Live Bacteria Using a Fluorogenic Silicon Rhodamine-binding Aptamer. Bio-protocol, 2020, 10, e3603.	0.2	1
377	A data collection system for protein crystallography with areaâ€sensitive proportional counters. Review of Scientific Instruments, 1991, 62, 1063-1066.	0.6	0
378	Constant volume gas thermometer without mercury. American Journal of Physics, 1994, 62, 666-667.	0.3	0

#	Article	IF	CITATIONS
379	Protein Dynamics from Intramolecular Electron Transfer. Materials Research Society Symposia Proceedings, 1996, 455, 337.	0.1	0
380	Conformational motions in the rugged energy landscape of proteins. , 1999, , .		0
381	Sub-10 nm Gold Nanoarrays for Tethering Single Molecules. Materials Research Society Symposia Proceedings, 2001, 676, 441.	0.1	0
382	Evidence for non-separating four-point correlation functions from IR pump-probe spectroscopy of CO in a protein internal cavity. Springer Series in Chemical Physics, 2005, , 631-633.	0.2	0
383	Bologna reforms in Germany. Physics Today, 2010, 63, 10-11.	0.3	0
384	Inside Cover: Structural Identification of Spectroscopic Substates in Neuroglobin (ChemPhysChem) Tj ETQq0 0 0	rgBT /Ove	erlock 10 Tf 5

385	High Resolution Microscopy in Live-Cell Imaging. Biophysical Journal, 2011, 100, 141a.	0.2	0
386	Protein Adsorption onto FePt Nanoparticles Investigated by Dual-Focus Fluorescence Correlation Spectroscopy. Biophysical Journal, 2012, 102, 401a.	0.2	0
387	Mechanism of Photo-Switching in mIrisGFP. Biophysical Journal, 2012, 102, 269a.	0.2	0
388	Spectroscopic Studies of Substrate and Ligand Binding in Inducible Nitric Oxide Synthase. Biophysical Journal, 2012, 102, 272a.	0.2	0
389	Uptake of Ultrasmall Fluorescent Gold Nanoclusters by Live Hela Cells. Biophysical Journal, 2013, 104, 161a.	0.2	0
390	Mechanistic Insights into Reversible Photoactivation in Proteins of the GFP Family. Biophysical Journal, 2013, 104, 681a.	0.2	0
391	Co Recombination in Human IDO and TDO - A Comparison. Biophysical Journal, 2014, 106, 676a.	0.2	0
392	STED-RICS - A Versatile Method for Studying Biomolecular Dynamics in Live Cells. Biophysical Journal, 2014, 106, 204a.	0.2	0
392 393		0.2 0.2	0
	2014, 106, 204a. Study of Receptor-Ligand Interactions in Living Specimens by using Dual-Color Dual-Focus		
393	2014, 106, 204a. Study of Receptor-Ligand Interactions in Living Specimens by using Dual-Color Dual-Focus Line-Scanning FCS. Biophysical Journal, 2015, 108, 324a.	0.2	0

#	Article	IF	CITATIONS
397	mGarnet, A Far-Red Fluorescent Protein for Live-Cell Sted Imaging. Biophysical Journal, 2016, 110, 488a.	0.2	0
398	Fluorescent Proteins for Super-Resolution Microscopy. Biophysical Journal, 2017, 112, 453a.	0.2	0
399	Single Molecule Imaging Reveals Dysferlin-Mediated Recruitment of Phosphatidylserine in Cell Membrane Repair. Biophysical Journal, 2017, 112, 146a-147a.	0.2	0
400	Energy Landscape Analysis of the Full-Length SAM-I Riboswitch using Single-Molecule FRET Spectroscopy. Biophysical Journal, 2018, 114, 684a-685a.	0.2	0
401	Primed Green-to-Red Photoconversion of Fluorescent Proteins Occurs via a Triplet State. Biophysical Journal, 2018, 114, 533a.	0.2	0
402	A Kinetic Study of Ligand Binding and Conformational Changes in Inducible Nitric Oxide Synthase. Biophysical Journal, 2019, 116, 65a-66a.	0.2	0
403	Line-Scanning Spatial Correlation Spectroscopy for Studying Dynamics in Biomembranes. Biophysical Journal, 2019, 116, 135a.	0.2	0
404	Wavelet-Based Background and Noise Removal for Fluorescence Microscopy Images. Biophysical Journal, 2021, 120, 359a.	0.2	0
405	Axial Line-Scanning STED-FCS. Biophysical Journal, 2021, 120, 182a.	0.2	0
406	OBSERVING CONFORMATIONAL CHANGES OF INDIVIDUAL RNA MOLECULES USING CONFOCAL MICROSCOPY. , 2001, , .		0
407	Functional relaxation determined by protein kinetics. Acta Crystallographica Section A: Foundations and Advances, 2004, 60, s124-s124.	0.3	0
408	Nonequilibrium 2D-IR Exchange Spectroscopy: Ligand Migration in Proteins. , 2006, , .		0
409	Granzyme B Produced by Human Plasmacytoid Dendritic Cells Suppresses T Cell Expansion Blood, 2009, 114, 2674-2674.	0.6	0
410	CD40 Ligand Determines Whether Interleukin 21 Induces Differentiation of Human B Cells Into Plasma Cells or Into Granzyme B-Secreting Cytotoxic Cells Blood, 2009, 114, 2675-2675.	0.6	0
411	Interleukin 21 can induce granzyme Bâ€secreting cytotoxic B lymphocytes. FASEB Journal, 2010, 24, lb506.	0.2	0
412	Incompletely activated CD4+ T cells induce granzyme B+ regulatory B cells in an interleukin 21â€dependent manner. FASEB Journal, 2010, 24, lb507.	0.2	0
413	A role for câ€Jun Nâ€terminal kinases in apoptosis triggered in human macrophages by carboxydextranâ€coated superparamagnetic iron oxide nanoparticles. FASEB Journal, 2010, 24, 520.3.	0.2	0
414	Incompletely Activated CD4+ T Cells Induce Granzyme B+ Regulatory B Cells In An Interleukin 21-Dependent Manner. Blood, 2010, 116, 3905-3905.	0.6	0

#	Article	IF	CITATIONS
415	Differential uptake of functionalized polystyrene nanoparticles by human macrophages and monocytic cells. FASEB Journal, 2012, 26, 580.9.	0.2	0
416	Photoenol Laser Lithography Using Intermediate-State Cis-Trans Isomerization for Writing Inhibition. , 2016, , .		0
417	Pax6 organizes the anterior eye segment by guiding two distinct neural crest waves. , 2020, 16, e1008774.		0
418	Pax6 organizes the anterior eye segment by guiding two distinct neural crest waves. , 2020, 16, e1008774.		0
419	Pax6 organizes the anterior eye segment by guiding two distinct neural crest waves. , 2020, 16, e1008774.		0
420	Pax6 organizes the anterior eye segment by guiding two distinct neural crest waves. , 2020, 16, e1008774.		0
421	Pax6 organizes the anterior eye segment by guiding two distinct neural crest waves. , 2020, 16, e1008774.		0
422	Pax6 organizes the anterior eye segment by guiding two distinct neural crest waves. , 2020, 16, e1008774.		0